Modeling and Simulation of the Apache Rotor System in CAMRAD II

Donald L. Kunz
Associate Professor
Old Dominion University
Norfolk, VA

and

Henry E. Jones
Aerospace Engineer
U.S. Army Aeroflightdynamics Directorate
Joint Research Program Office
NASA Langley Research Center
Hampton, VA

Abstract

The unique capabilities of CAMRAD II are used to develop two enhanced models of the AH-64 Apache rotor system. Based on existing sources of structural and dynamic blade properties, common characteristics of both models are first validated. Then, a single-load-path, kinematic joint model, which includes the exact kinematics of the blade retention system, is developed and validated. A multiple-load-path model, which incorporates an accurate representation of the strap pack into the kinematic joint model, is also created. Pitch link loads are calculated and compared to flight test data.

Introduction

The purpose of creating an analytical model of any helicopter rotor system is to facilitate accurate prediction of blade response and loads under a variety of flight conditions. For a mature design, like the AH-64 Apache rotor system, these predictions may be used for evaluating flight conditions for which no flight test data exists, or as a baseline for proposed enhancements to the rotor system design. Prior to the work described herein, two validated models of the Apache rotor were in general use. The first, and oldest, is a model originally developed by Hughes Helicopter Company, and now maintained by Boeing-Mesa (formerly McDonnell Douglas), which is implemented using a proprietary computer program known as DART (Dynamic Analysis Research Tool)[1]. The other model was also developed at Boeing-Mesa, and is implemented using CAMRAD/JA (Comprehensive Analytical Model of Rotorcraft Aerodynamics and Dynamics/Johnson Aeronautics).

Since two validated models of the Apache rotor are currently in use, one could reasonably ask if a new model is necessary. In fact, a new model of the Apache rotor blade can be justified by looking at the weaknesses of DART and CAMRAD/JA. DART is a finite difference dynamics analysis code written by Dr. Richard McNeal in the 1960's. Although it has been upgraded several times, the aerodynamic model is crude, and the structural model allows for only 15 lumped-parameter elements on a single blade. It does, however, support multiple load paths and piecewise constant or piecewise linear input for structural properties. CAMRAD/JA, on the other hand, makes use of modal methods for structural modeling and supports sophisticated aerodynamic models. It does not, however, support multiple load paths. Input of structural properties in CAMRAD/JA is also limited to 100 stations, and the properties between those stations are assumed to be piecewise linear. Since integrals involving the blade properties are always calculated using 51 equally spaced stations (independent of the input stations), integrals of the input properties as calculated by CAMRAD/JA may not yield the same results as the exact integrals.

The models of the Apache rotor system described herein were developed using CAMRAD II, a descendent of CAMRAD/JA, but with greatly enhanced modeling capabilities. CAMRAD II supports multiple load paths, sophisticated aerodynamic and structural models, and improved methods for evaluating integrals of blade properties. Therefore, the use of CAMRAD II for the analysis of the Apache rotor system brings improved analytical methods to the modeling process.

The Apache rotor system is unique among modern helicopter rotor systems in that, strictly speaking, its design is neither fully articulated, nor hingeless, nor bearingless. Instead, it contains features that are common to all three design concepts. For example, it does have a true lag hinge like an articulated rotor; but like a hingeless rotor, there is no true flapping hinge. However, as in many bearingless designs, pitch is input

through a pitch housing that twists a flexible member (the strap pack in this case). Pitching kinematics are then restrained in both bearingless designs and the Apache rotor by a "snubber" mechanism. As a result of the hybrid nature of the Apache rotor system, accurate modeling of the kinematics in CAMRAD II is not a trivial task, but rather is one that requires a detailed knowledge of the structure and kinematics of the rotor system.

This paper first discusses issues that must be addressed when modeling the Apache rotor in CAMRAD II, or any other comprehensive rotorcraft analysis code. In addition to the kinematics of the blade restraint and pitch control, issues relating to the definition of blade inertial and elastic properties that are input to CAMRAD II are discussed. Then, the paper describes the development of two enhanced blade models. The first model is a single-load-path, kinematic joint model that improves on the baseline blade model by incorporating the exact kinematics of the blade retention system. It does not attempt to model the strap pack, but instead uses equivalent springs to simulate the presence of the strap pack. The second model improves upon the first model by eliminating the equivalent springs and including a structurally accurate strap pack model. Validation of both rotor models is performed using *in vacuo*, isolated blade natural frequencies and modeshapes. The capabilities of the enhanced Apache blade models are demonstrated by comparing simulations from CAMRAD II with flight test data.

Main Rotor Blade Properties

Three sources are available for obtaining definitions of the Apache main rotor blade properties: (1) the input decks for existing CAMRAD/JA models; (2) the U.S. Army ADS-10B Air Vehicle Technical Description[2]; and (3) a McDonnell Douglas technical report[3] that includes a detailed description of the AH-64A main rotor. Of the three sources, the latter two were the most useful, for the reasons described below.

CAMRAD/JA Model Data

The structural properties that are used in any of the CAMRAD/JA models of the Apache blade are primarily derived from the input data for the DART model. Those properties are principally based on measured properties of the blades. Since the input used in CAMRAD/JA is derived from another source (DART), it is not used herein as a principal source for the definition of the CAMRAD II input properties. As a note to anyone wishing to examine one of the several CAMRAD/JA models in existence, the number and locations of the input stations can be used as a guide to the source of the property data. If the model defines properties at exactly 51 equally spaced stations, the properties most likely have been averaged to produce accurate integrals and do not (in some areas) accurately reflect the actual blade properties. Other distributions of the input properties are probably derived directly from the DART properties, and are fairly accurate representations of the true blade properties. However, if these properties are used as input to CAMRAD/JA some of the blade integrals will be inaccurate, an may have some affect on the results obtained from the analysis. Table 1 lists the blade structural properties used in CAMRAD/JA and their definitions.

Table 1. CAMRAD/JA Blade Properties

Property	Definition (Units)
EIXX	Flap bending stiffness (lb-ft^2)
EIZZ	Lag bending stiffness (lb-ft^2)
GJ	Torsion stiffness (lb-ft^2)
IPOLAR	Polar moment of inertia (slug-ft)
ITHETA	Moment of inertia (slug-ft)
KP2	Polar radius of gyration squared
MASS	Mass (slug/ft)
TWISTI	Blade twist (degrees)
XC	Tension center offset
XI	Center of gravity offset

ADS-10B Data

The Air Vehicle Technical Description (ADS-10B)[2] is a U.S. Army document that was developed by McDonnell Douglas Helicopter Company during the early stages of the Longbow Apache development. This document contains a complete description of the aircraft. Table 2 lists the structural properties of the main rotor blade, as tabulated in the ADS-10B. With regard to the main rotor blade properties, the values provided in the document are based primarily on input to the DART model developed by McDonnell Douglas Helicopter Company. The properties based on the DART input can be directly related to the measured properties of the blade. Some of the properties listed in Table 2 are attributed to the CAMRAD/JA model used by McDonnell Douglas. These properties were not required as input to DART, but were required as input to CAMRAD/JA and by the ADS-10B. Blade properties based solely on CAMRAD/JA input data were not used herein to define CAMRAD II input data, unless they could be independently verified.

With regard to the properties in the ADS-10B (Table 2) and the properties used for the CAMRAD II model, there are several potential problems that should be noted. First, for the swept tip portion of the blade, all values referenced to the leading edge of the blade in the ADS-10B are referenced to the extended leading edge of the straight portion, not to the physical leading edge of the swept tip. The units listed for the flapwise, chordwise, and torsion stiffnesses, and the polar moment of inertia in the ADS-10B are incorrect. The correct units are shown in Table 2. The location of the feathering axis in the ADS-10B is incorrect. It should be 5.67 inches aft of the leading edge (and leading edge extended). The location of the shear center (elastic axis) between Stations 49.5 and 271.7 in the ADS-10B is also incorrect. Measurements made at Boeing-Mesa subsequent to the release of the ADS-10B have shown that it is actually 5.04 inches aft of the leading edge.

McDonnell Douglas Data

The principal value of the data in Reference 3 is that it defines the geometry and properties of the components inboard of the lag hinge (Station 39.5). These values are vital in order to create a model that accurately simulates the kinematics of the components at the blade root. Of particular importance are the structural properties of the strap pack and pitch housing, which are needed to create an accurate model of the blade retention system.

Single-Load-Path Joint Model

In this section, the geometry and structural properties of the single-load-path, kinematic joint model of the Apache main rotor blade are described. The CAMRAD II model created from these properties is then compared to the full-scale blade. As noted above, the structural properties for the model were selectively obtained from the ADS-10B and Boeing-Mesa data, then independently checked for accuracy.

Main Rotor Blade Geometry

CAMRAD II provides several facilities that allow the main rotor blade model to accurately reflect the kinematics and dynamics of the full-scale blade. The most important of these facilities are the finite-element beam segments and the joint connections. In order to facilitate comparisons with existing models, a baseline single-load-path model of the main rotor blade was created using the automated facilities in the Rotorcraft Shell provided by CAMRAD II. Subsequent sections describe the creation of the single-load-path, kinematic joint model.

Blade Segment Definitions

The single-load-path blade defined by the Rotorcraft Shell in CAMRAD II automatically locates beam segment boundaries based on the locations of the flap and lag hinges, the pitch bearing, and the blade tip. On the Apache blade, the flap hinge and pitch bearing are collocated at Station 11.0, the lag hinge is located at Station 34.5, and the tip is located at Station 288.0. One approach that could be used to define the beam segment boundaries is to follow the approach used by CAMRAD/JA. Under that approach, the true locations of the flap and lag hinges is defined in the input data, and the pitch bearing is defined to be slightly outboard of the flap hinge. In that case, CAMRAD II automatically creates a finite-element beam that extends from the hub center to the flap hinge (Station 11.0), and a very short beam element between the flap hinge and pitch bearing (e.g., Station 11.03). Finally, another beam element is created between the pitch bearing and the lag hinge (Station 34.5).

The disadvantages of CAMRAD/JA approach to defining the inboard beam segments are that the blade is not kinematically accurate, and the enhanced modeling capabilities of CAMRAD II are not put to use. In order to create a kinematically accurate model of the blade, the flap hinge and pitch bearing must be coincident. Therefore, in this enhanced model, the blade is defined in the Rotorcraft Shell to have a pitch bearing at Station 11.0 and no flap hinge. The Core Input capabilities of CAMRAD II allow the pitch-flap bearing to be created later by modifying the pitch bearing initially defined in the Rotorcraft Shell. The reason for defining the pitch bearing rather than the flap hinge is to permit the pitch control mechanism to be set up automatically by CAMRAD II. Thus, inboard of the lag hinge, the endpoints of the blade segments are located at blade stations 11.00 and 34.50.

Outboard of the lag hinge, the blade must be manually divided into segments. Since CAMRAD II requires the reference axis of each beam segment to be linear, the swept tip section of the blade must be modeled with a beam element of its own. This beam segment extends from Station 271.7 to the tip of the blade (Station 288). Since the blade properties are constant over a large portion of the blade (Stations 104 - 232), it is reasonable use nearby stations as element boundaries. However, since the constant section encompasses more than 40% of the blade, it is divided into two equal segments. Between the lag hinge and the beginning of the constant section, two segments of unequal length are also defined, based on the distribution of blade properties just outboard of the lag hinge and the fact that much of the beam bending takes place in that region. The complete single-load-path blade model therefore consists of eight finite-element beam

segments. The endpoints of these segments are located at blade stations 11.00, 34.50, 63.00, 108.00, 162.00, 216.00, 271.70, and 288.00.

Joint Definitions

The default behavior of the Rotorcraft Shell is to model the flap hinge, pitch bearing, and lag hinge as individual, one-degree-of-freedom joints. As described above, the pitch-flap bearing, which is located at Station 11.0 is not a one-degree-of-freedom joint. It is, in fact, a single elastomeric bearing, which has four degrees of freedom (three rotations and axial translation), that connects the pitch housing to the rotor hub.

In order to model the true kinematics of the pitch-flap bearing, Core Input is used to modify the definition of the pitch bearing, as defined by the Rotorcraft Shell. The one-degree-of-freedom pitch bearing is redefined to be a ball joint with an additional axial displacement degree of freedom. The -4° of droop present in the full-scale blade is not modeled. Equivalent springs are included to simulate control system (pitch) stiffness, and strap (axial, flap, and lag) stiffness. The stiffness of the control system spring is based on data contained in Reference 3, while the axial and lag stiffnesses are based on a simple finite-element model[4] of the strap.

Blade Properties

In CAMRAD/JA, the rotor blades consist of a single beam element having a straight elastic axis, and the blade properties are integrated using 51, equally spaced, blade stations. This integration method has a problem, in that large changes in blade properties between the blade stations may be lost. Therefore, in order to assure that CAMRAD/JA evaluates the integrals accurately, they must first be calculated independently. Then, the property definitions in CAMRAD/JA must be adjusted to yield the correct integrals. In cases such as blade mass distribution, which is used to calculate blade moments of inertia as well as blade mass, it may be difficult or even impossible to obtain correct values for all of the integrals.

CAMRAD II improves on the integral evaluations by calculating the integrals for each blade segment using Gaussian quadrature. The default number of Gauss points for each beam element is 4, and linear interpolation is used to determine property values at the Gauss points. Ideally, one would like to use a large number of Gauss points for those beam elements that contain large gradients in their property distributions, then define the properties at each of the Gauss points. In addition to being a tedious process and one prone to error, this approach obscures the true blade property distributions. The method chosen for this model was to use the true blade property distributions as input, and then use the maximum number of Gauss points (20) in each beam element to evaluate the integrals. It possible to use Core Input to reduce the number of Gauss points in the uniform beam segments, but the computational advantage is not believed to be sufficient to justify the effort.

Blade Properties Outboard of the Lag Hinge

The principle reason that none of the alternatives described above are ideal is that CAMRAD II requires that all of the structural (and aerodynamic) blade properties be defined at the same set of blade stations. Figure 1 shows the distribution of blade stations for each of the blade structural properties, as defined in the ADS-10B. Therefore, the selection of blade stations at which the blade properties should be defined is an issue that must be addressed. In addition, the properties in the region of the swept tip require special attention.

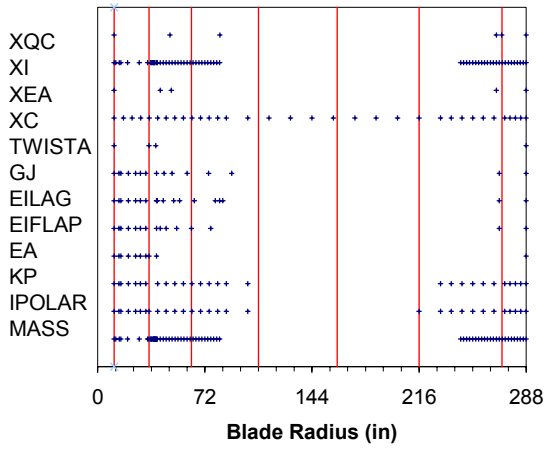

Figure 1. Distribution of Blade Structural Properties

As noted above, the properties of the Apache main rotor blade are constant over a large portion of the blade (Stations 104 - 232). However, in the regions near the blade root and the blade tip, the properties are subject to large variations. In those regions of large property variations, the stations at which the properties are defined are more closely spaced than in the uniform section (Figure 1). In order to accommodate the different blade station distributions for the various properties, the input data defines each property at all stations. If a particular property is not defined at a specified station, its value is determined by interpolation. For all properties except blade mass and center of gravity, which are piecewise constant, property values are calculated using linear interpolation.

The CAMRAD/JA model of the blade and the ADS-10B define the chordwise center of gravity, the chordwise tension center, and the polar radius of

gyration with respect to the elastic axis, which is assumed to be straight over the entire length of the blade. In CAMRAD II, the use of finite-element blade segments (within which the elastic axis must also be straight) permits an elastic axis that is not necessarily straight over the entire length of the blade. Therefore, in the swept tip region of the blade, those properties that were defined in the ADS-10B for a straight elastic axis must be modified to account for the swept elastic axis in CAMRAD II.

Inboard of the Lag Hinge

A single-load-path blade model is not capable of modeling the strap pack and pitch case separately. Therefore, the properties of the two structures are combined in this model. In order to verify the properties listed in the ADS-10B, the individual properties of the components, as listed in Reference 3, are used. A couple of anomalies are noted and corrected in the final blade properties.

First, it appears that the mass of the lag dampers is added twice in the CAMRAD/JA model. This error probably resulted from the bookkeeping method required for the DART model, which categorizes all components as either contributing to the flap or lag inertia (or both). In the case of the lag dampers, part of the damper mass is lumped into the flap inertia, and part is lumped into the lag inertia. It appears that when the CAMRAD/JA model was created, the distributed mass of the dampers was added as well. Another possible explanation for this error is that the flap and lag masses from the DART model were simply added when creating the mass distribution for the CAMRAD/JA model. This would also result in some mass being included twice.

The second anomaly is associated with the ADS-10B flapwise stiffness properties, chordwise stiffness properties, and radius of gyration near the lag hinge. In most CAMRAD/JA models, the property data indicates a soft spot in the vicinity of the lead-lag link, which is, in reality, made of titanium and is exceedingly rigid. Uncorrected, the soft spot in the property distribution results in erroneous values of the fundamental flap and lag frequencies. The error is due to the calculation of the moment of inertia of the pitch housing at the point where it attached to the lead-lag link. Due to the shape and cross-section of the pitch housing, in that vicinity, the moments of inertia are small. However, the lead-lag link overlaps the hinge area, which results in a very stiff structure. It was verified that the CAMRAD II model described herein does not have this problem.

Validation

The baseline configuration used for the validation of the single-load-path kinematic joint model is the single-load-path model that was created by a direct translation of the input data from CAMRAD/JA to CAMRAD II. A series of intermediate configurations, leading to the single-load-path model with a true pitch-flap bearing, were also created. The first intermediate configuration (Joint-P) was created from the baseline model by eliminating the flap hinge moving the pitch bearing to its proper location. A flapping degree of freedom was added to obtain the second configuration (Joint-PF), and a lag degree of freedom was added to get the third configuration (Joint-PFL). The complete kinematic joint (Joint), with pitch, flap, lag, and axial degrees of freedom was finally created by adding the axial degree of freedom to the Joint-PFL configuration. The *in vacuo*, isolated blade natural frequencies calculated for these configurations are compared in Table 3, along with the collective and cyclic natural frequencies calculated by DART and tabulated in the ADS-10B.

The characteristics of the four-degree-of-freedom (4DOF) model of the pitch-flap bearing can be explained by a close examination of Table 3. A comparison of the baseline frequencies in column 1 and the pitch joint in column 2 of Table 3 shows that the flapping frequencies for the baseline configuration (1.030, 2.714, 4.859, 7.968) are shifted upwards (1.193, 3.368, 6.653, 10.749) when the flap hinge is removed. All other modal frequencies remain relatively unchanged. When the joint flapping degree of freedom is reintroduced in the joint, the flapping frequencies in columns 3 through 5 return to values close to the baseline frequencies. The addition of the lag degree of freedom to the joint (column 4) results in a decrease of the lag frequencies, since lag flexibility is introduced inboard of the lag hinge. However, this change improves correlation with the rigid cyclic lag mode from the ADS-10B, as compared with the baseline configuration. It should also be noted that the lag degree of freedom and the associated spring introduce a highly damped local mode near 6/rev (not shown in Table 3). This mode was determined to be an out-of-phase motion of the pitch housing and blade, and can be eliminated by arbitrarily increasing the lag spring stiffness. The addition of the axial degree of freedom (column 5) does not have a significant effect on the blade frequencies, but was found to correctly predict the equivalent strap stretch under centrifugal load.

It should be noted that the ADS-10B is the most authoritative source available for the Apache rotor frequencies, since experimental verification of the rotor frequencies is not well documented. The designations of collective and cyclic modes in Table 3 refer to the boundary conditions imposed by the DART model. For single blade analysis, it is most appropriate to compare flapping modes to the collective modes in flap, and lag modes to the cyclic modes in lag. Some experimental

measurements of blade frequencies were made during whirl tower testing of the Apache rotor. Resonant frequencies encountered during the sweeps were extrapolated to 100% normal rotor speed. Those measurements show the first flap bending frequency at 2.80/rev, the pitch frequency between 4.05/rev and 4.14/rev, the second flap bending frequency at 4.89/rev, and the first chord bending frequency at 6.55/rev[5].

Multiple-Load-Path Strap Model

As described above, the single-load-path, kinematic joint model of the Apache main rotor blade places the pitch-flap bearing at Station 11.0. The lag hinge is then located at Station 34.5. Finite-element beams, which extend from the hub center to the flap hinge and then from the pitch bearing to the lag hinge, are created by CAMRAD II. For this model, a four-degree-of-freedom joint model with equivalent springs is used to simulate the kinematics of the pitch-flap bearing as well as the flexibility of the strap pack. The following paragraphs describe the development and validation of a multiple-load-path model that incorporates a structural model of the strap pack using finite-element beams.

Strap Pack Structural Model

The strap pack on the Apache main rotor blade is the primary structural component for carrying centrifugal loads. Geometrically, it is shaped like a "Y", where the inboard ends of the two legs are attached to the rotor hub and the outboard end of the throat is pinned to the lag hinge (Figure 2). It should be noted that at the lag hinge, all three components that come together at that point (pitch housing, strap pack, and lead-lag link) are pinned together, and can rotate independently of one another.

The strap pack model itself consists of the two legs and the throat, modeled by three finite-element beams. The legs of the strap model are attached to the rotor hub at Station 7.00, where the lateral coordinates are 4.686 inches fore and aft of the feathering axis. The legs, making an angle of 9.5° with respect to the feathering axis, extend out to Station 28.80, at which point their lateral coordinates are 1.038 inches fore and aft of the feathering axis. (Note that if the centerlines of the legs are extended, they will intersect at Station 35.00.) The throat begins at Station 28.80 and extends to Station 34.50, where it is pinned to the lag hinge. The elastic axis of the throat is collinear with the feathering axis.

The strap pack is made up of 22 laminates of 0.014-inch thick, AM355 stainless steel, and the structural and inertial properties are calculated using the appropriate geometry and material properties (Ref. 3). Initially, the cross-section moments of inertia in the flapping direction were calculated to include the offset of each laminate from the centerline of the leg or throat. Using this method of calculation results in the same cross-section moments of inertia that one would calculate for a single metal strap 0.308 inches thick. As a result, the calculated flapping stiffness and the natural frequencies turn out to be significantly greater than the expected values. Therefore, in the final model, the offset is neglected in the calculation of the moment of inertia. Values of the chordwise moment of inertia are not affected by the offset, and there is little effect on the polar moment of inertia, since it is dominated by the chordwise moment of inertia. The definitions of the structural properties of the strap also take into account the presence of the "shoes" at each end of the strap. These shoes restrict the flap bending and torsion motions of the strap, but do not affect the lag bending or axial motions. Therefore, the values of flap stiffness and torsion stiffness are arbitrarily multiplied by a factor of 10 for the portions of the strap that are under the shoes.

In this model, the inboard ends of the leading-edge and trailing-edge strap leg finite-element beams are rigidly attached to the rotor hub. The outboard ends of the leading-edge and trailing-edge strap legs are rigidly attached to the inboard end of the throat. The outboard end of the throat is, in turn, pinned to the outboard end of blade element 2, the pitch housing.

Validation

Comparisons of the *in vacuo*, isolated blade natural frequencies of the strap pack model with the natural frequencies of the kinematic joint model, the baseline CAMRAD/JA model, and the ADS-10B collective and cyclic modes are shown in Table 4. The table shows that the addition of the strap model into the blade retention system has introduced two significant changes in the natural frequencies. First, the lag frequencies have increased, as compared to the joint model, due to the stiffening influence of the strap. The rigid lag mode frequency increased from 0.502 in the joint model to 0.528, and the first flexible lag mode frequency increased from 6.108 to 6.570. Apparently, the equivalent lag spring in the kinematic joint model is too soft, as compared to the strap modeled with finite-element beams. As a result of the stiffened lag modes, the frequency of the highly damped, out-of-phase mode (not shown in Table 4), which was observed in the joint model, has more than doubled. Second, the rigid pitch mode frequency, which was near 4/rev for both the joint model and baseline model increased slightly to approximately 4.15/rev.

In addition to an examination of the modal frequencies at 100% normal rotor speed, it is instructive to look at a

fan plot of the blade frequencies (Figure 3). From this figure, it is much easier to associate the blade modes with the flap, lag, and pitch motions of the blade. Figure 3 shows that the natural frequencies calculated using all three models are in very good agreement throughout the frequency range. The only significant exception is the first flexible lag mode from the joint model. The natural frequencies of that mode are significantly lower than those calculated by either the baseline or strap models.

Pitch Link Loads Calculations

One of the primary objectives for creating the enhanced models of the Apache rotor blade, including a kinematically accurate blade retention system and a strap pack model, is to improve the predictive capability of the model in general. To that end, sample calculations of pitch link loads are performed using both the baseline and kinematic joint models. Pitch link loads are notoriously difficult to predict and the baseline model, which is a single-load-path model, makes no attempt to model the blade retention kinematics accurately. The joint model, on the other hand endeavors to model the kinematics of blade retention accurately, but uses only equivalent springs in place of the strap pack.

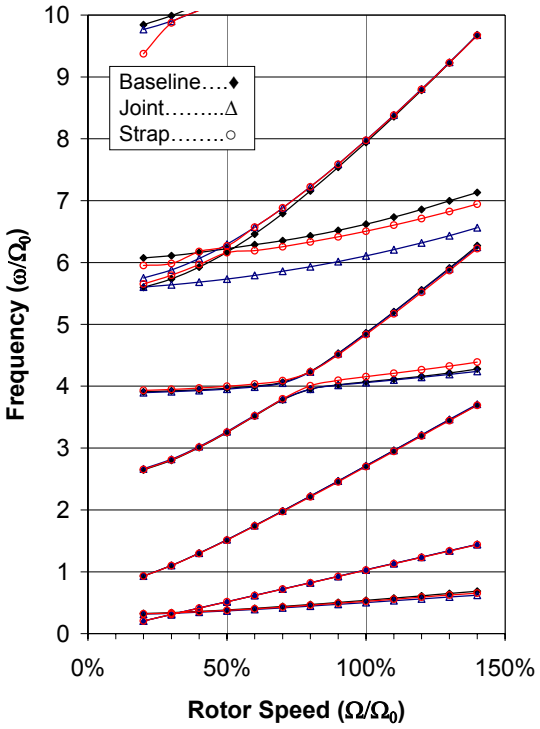

Figure 3. Apache Fan Plot

The flight condition chosen for these calculations is steady, level flight, and the parameters are shown in Table 5. For all of the calculations that follow, the CAMRAD II solutions were obtained under the free flight trim option. All solutions were calculated using 8 harmonics and 64 azimuth stations. The number of harmonics was increased from the nominal value of 4, in an attempt to capture some of the higher harmonic response observed in the flight test data. With the increase in the number of harmonics, the number of azimuth stations also had to be increased. The maximum number of stations that could be used without modifications to CAMRAD II is 64 (for 8 harmonics). Superior results for the higher harmonic response may be obtained by using more azimuth stations.

Table 5. Flight Condition Parameters

Parameter	Value
Gross Weight	15305.8 lbs
C_W/σ	0.09744
Aircraft Speed	120.5 kts
Rotor Speed	289 rpm
Altitude	9713 ft MSL
Air Density	0.01774 slugs/ft^3
Temperature	23.86°F

Table 6. lists the converged trim control variables that were obtained for the baseline and kinematic joint models. Based on the agreement of these values, the trimmed conditions of both models are nearly equivalent, and acceptable for the purposes of comparison.

Table 6. Trim Control Variables

	Baseline	Joint
Collective Pitch	12.53°	12.42°
Lat Cyclic Pitch	-0.76°	-0.73°
Lng Cyclic Pitch	6.09°	6.33°
Pedal	-0.341°	-0.315°
Pitch	-1.75°	-1.74°
Roll	-4.01°	-3.90

The pitch link loads were first calculated using the baseline model. The results from calculations using uniform inflow, a prescribed wake, and a free wake are shown in Figure 4. It is obvious that the uniform inflow solution is inadequate for predicting the pitch link loads. Its predictions of both the mean and peak-to-peak loads are poor. The prescribed wake calculations and the free wake calculations yield results that are very close to one another, and are superior to the uniform inflow results. In particular, the prescribed wake and free wake calculations show the broad peak on the advancing side of the rotor disk and a deep valley on the retreating side that are not present in the uniform inflow results. However, neither yields particularly good results for either the mean or peak-to-peak values of the pitch link loads.

Another problem with the baseline calculations is the placement of the major peaks and valleys does not correlate well with the flight test data. The flight test data shows a broad peak between 40° and 90° of azimuth, while the broad peak in the calculations is between 80° and 140°. Also, the deep valley in the flight test data occurs at 270°, while the calculations predict it to be at 190°. This is not just a phasing problem, since the broad peak in the calculations lags the flight test data 40°, while the valley leads by 80°.

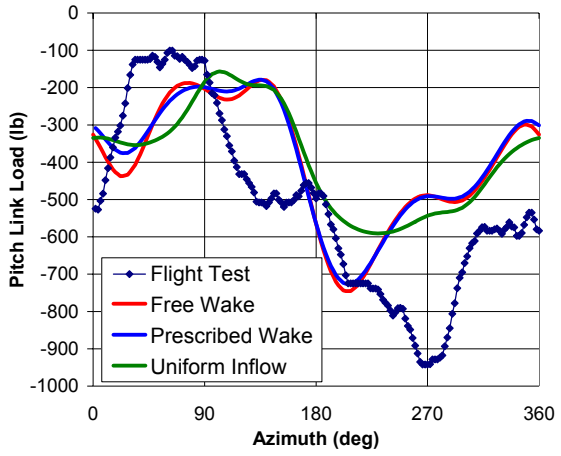

Figure 4. Pitch Link Loads: Baseline Model

Figure 5 shows a similar comparison of the results from the different wake models for the single-load-path, kinematic joint model. Again, the uniform wake load calculations are much different from those made using the prescribed wake and free wake. However, in this case, the uniform inflow model is observed to be superior to the other wake models in matching the mean load, and is marginally better in predicting the peak-to-peak load.

All three of the wake models predict a broad peak on the advancing side of the rotor disk, but like the baseline model, the placement lags the flight test data. Unlike the baseline model, none of the wake models used in the kinematic joint model show a deep valley on the retreating side.

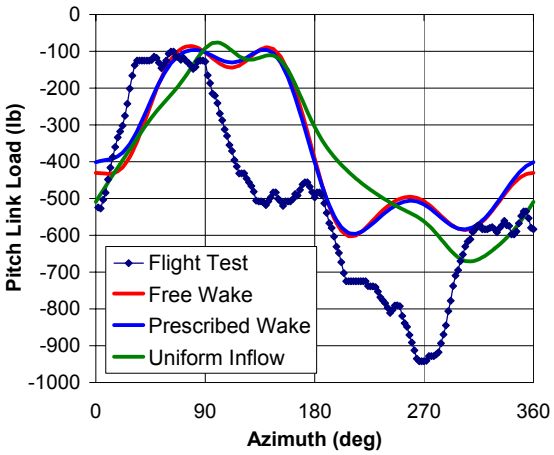

Figure 5. Pitch Link Loads: Kinematic Joint Model

The results from the free wake calculations for the baseline and kinematic joint models are compared to the flight test data in Figure 6. The kinematic joint model appears to be superior to the baseline model on the advancing side, while the baseline model is somewhat superior on the retreating side. Clearly, neither model shows exceptional predictive capabilities with respect to pitch link loads.

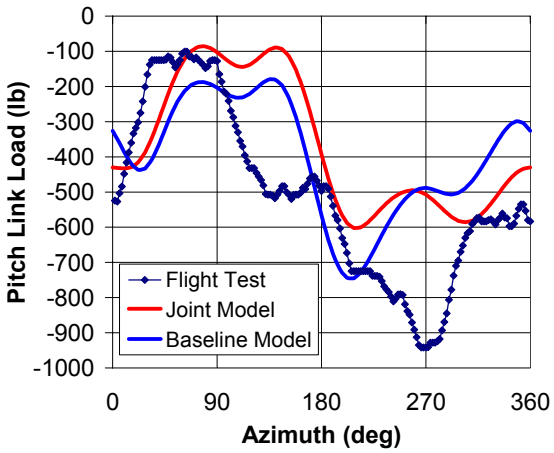

Figure 6. Pitch Link Loads: Free Wake Models

Concluding Remarks

Two new, enhanced models of the Apache rotor system, a single-load-path model and a multiple-load-path

model have been created for CAMRAD II. The single-load-path, kinematic joint model is an improvement over the existing, single-load-path, baseline model in that it accurately models the kinematics of the blade retention system. The multiple-load-path model improves upon the kinematic joint model by including a finite-element beam model of the strap pack.

The *in vacuo*, isolated blade natural frequencies for both models have been validated against a standard set of frequencies that are generally accepted to be representative of the natural frequencies of the Apache rotor system. Both the kinematic joint model and strap pack model showed excellent correlation. However, the lack of well-defined dataset of experimental measurements against which the models may be validated is disappointing.

Pitch link loads were calculated for a straight and level flight condition, and compared to available flight test data. The results from the kinematic joint model appear to be marginally better than the results from the baseline model, which indicates that the accurate modeling of blade retention kinematics alone is probably not a major factor in obtaining accurate pitch link loads.

Future work in this area will include using the multiple-load-path, strap pack model to calculate strap loads, as well as pitch link loads. These calculations are not included herein due to major difficulties in getting the strap pack model to trim and generating the Core Input needed to calculate the strap loads.

References

[1] Elliott, A.S., "DART Users Manual," McDonnell Douglas Helicopter Company, Flight Technology Technical Note, FTN 88-017, October 1988.

[2] Taylor, H.E., "Longbow Apache Air Vehicle Technical Description," McDonnell Douglas Helicopter Company, December 1991

[3] Straub, F.K., "AH-64A Main Rotor Model Documentation," Flight Technology Technical Note, FTTN-95-001, McDonnell Douglas Helicopter Company, February 1995.

[4] Reddy, J.N., Introduction to the Finite Element Method, 2nd Edition, McGraw Hill, 1993, Chapter 7.

[5] Silverthorn, L.J., Private communication, September 2000.